Effects of Mesogenic Shape and Flexibility on the Phase Structures of Mesogen-Jacketed Liquid Crystalline Polymers with Bent Side Groups Containing 1,3,4-Oxadiazole

Yiding Xu, Qian Yang, Zhihao Shen,* Xiaofang Chen, Xinghe Fan,* and Qifeng Zhou*

Beijing National Laboratory for Molecular Sciences, Key Laboratory of Polymer Chemistry and Physics of Ministry of Education, College of Chemistry and Molecular Engineering, Peking University, China

Received January 20, 2009; Revised Manuscript Received February 21, 2009

ABSTRACT: We report the design, synthesis, and characterization of a new series of mesogen-jacketed liquid crystalline polymer (MJLCP) with rigid bent-core side groups and different flexible tails. The structures of monomers of 3,5-bis[(4-alkoxy-phenyl)-1,3,4-oxadiazole]styrene (MC_x, x is the number of carbons in the alkoxy groups, $x = 4$, 6, 8, 10, 12, 14, 16, and t for *tert*-butyl) were confirmed by ^{1}H NMR, mass spectrometry, IR, and elemental analysis. Basic characterizations of polymers were performed with ^{1}H NMR and gel permeation chromatography. The phase transition and structures of polymers were investigated via differential scanning calorimetry, wide-angle X-ray diffraction, and polarized light microscopy experiments. Hexagonal column (Φ_H) liquid crystalline phases with long-range order on a length scale of 3−5 nm and short-range order of 0.5 nm were observed in all PC_x while monomers had no liquid crystallinity. The flexible alkoxy side groups of polymer rods interpenetrated with others except for rigid *tert*-butyl groups. Compared with the reported work in our group, a change in substitute position resulted in totally different packing of both monomers and polymers. Namely, both the molecular shape and the flexibility may greatly affect the packing behaviors of polymers and thus their liquid crystalline phase structures.

Introduction

Phase structures and transitions of thermotropic liquid crystalline (LC) polymers have been one of the most important topics studied in polymer chemistry and physics for their various applications, such as optical devices and engineering plastics.[1] Based on the position of the mesogenic groups in the polymers, LC polymers can be classified into two classes, main-chain and side-chain LC polymers.[2] For side-chain LC polymers, the mesogenic groups can be either laterally or terminally attached to the polymer backbone. To improve the mobility of the mesogenic groups and facilitate the formation of LC phase structure, flexible spacers are needed between the mesogens and backbones.[3] In 1987, Zhou et al. proposed another type of side-chain LC polymers called "mesogen-jacketed liquid crystalline polymers" (MJLCPs) which had a very short spacer between the backbone the laterally attached mesogens.[4] From that time, several series of MJLCPs with no spacers between the backbone and the rod-like mesogens based on 2-vinylhydroquinone, 2-vinyl-1,4-phenylenediamine, 2-vinylterephthalic acid, and 2-vinyl-*p*-terphenyl were also synthesized and their LC phase behaviors were investigated.[5−14] Because of the strong steric interaction between mesogens, the polymer backbones are forced to adopt an extended-chain conformation as supramolecular rods to accommodate side groups.[15,16] Thus, most MJLCPs can form columnar LC phases, which are different from conventional side-chain LC polymers but similar to LC polymers containing disk-like mesogens.[17,18] Recently, three series of MJLCPs of poly-[4,4′-bis(4-butoxyphenyloxycarbonyl)-2-vinylbiphenyl] (PBP2VBP), poly[4,4′-bis(4-butoxyphenyloxycarbonyl)-3-vinylbiphenyl] (PBP3VBP), and poly{2,5-bis[(4-alkoxy-phenyl)-1,3,4-oxadiazole]styrene} were synthesized, and their LC phases of smectic A were identified.[19,20] In addition, Chen et al. first reported two series of bent-core MJLCPs, and columnar rectangular phases were observed.[21] So far, we know that both the molecular shape and the chemical structures can influence the packing of mesogens in polymer chains and thus their LC phase behavior.

To further investigate the relationship between molecular shape and polymer liquid crystalline phase structure, a series of poly{3,5-bis[(4-alkoxy-phenyl)-1,3,4-oxadiazole]styrene} (PC_x, x is the number of carbons in the alkoxy groups, $x = 4$, 6, 8, 10, 12, 14, 16, and t for *tert*-butyl) were synthesized. Here, bent side groups with a five-ring rigid part containing 1,3,4-oxadiazole and no linkage groups between the rings, were first laterally attached to the polymer backbone. The chemical structures of polymers are shown in Scheme 1.

As expected, all monomers and polymers had better solubility than those with rod-like mesogens. Our experiment results also suggested that PC_x could pack into well-defined hexagonal columnar LC phases. In addition, polymer rods with alkoxy tails of different flexibility, which include the fully rigid *tert*-butyl tail and flexible alkoxy tails (note the polymer backbone was surrounded by side groups), showed quite unusual d_{100} values. Thus, the surface property may more or less influence the packing of polymer chains.

Experimental Section

Materials. The compound *p*-alkoxybenzhyhydrazide was synthesized using the method previously reported.[19] Benzoyl peroxide (BPO) was purified by recrystallization from ethanol. Tetrahydro-

Scheme 1. Chemical Structures of Polymers

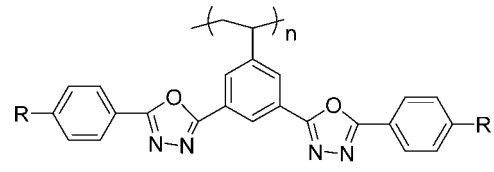

R = - OC_xH_{2x+1} , x = 4, 6, 8, 10, 12, 14, 16

R = -$C(CH_3)_3$

* To whom correspondence should be addressed. E-mail: (X.F.) fanxh@pku.edu.cn; (Z.S.) zshen@pku.edu.cn; (Q.Z.) qfzhou@pku.edu.cn.

10.1021/ma900125c CCC: $40.75
Published on Web 03/16/2009

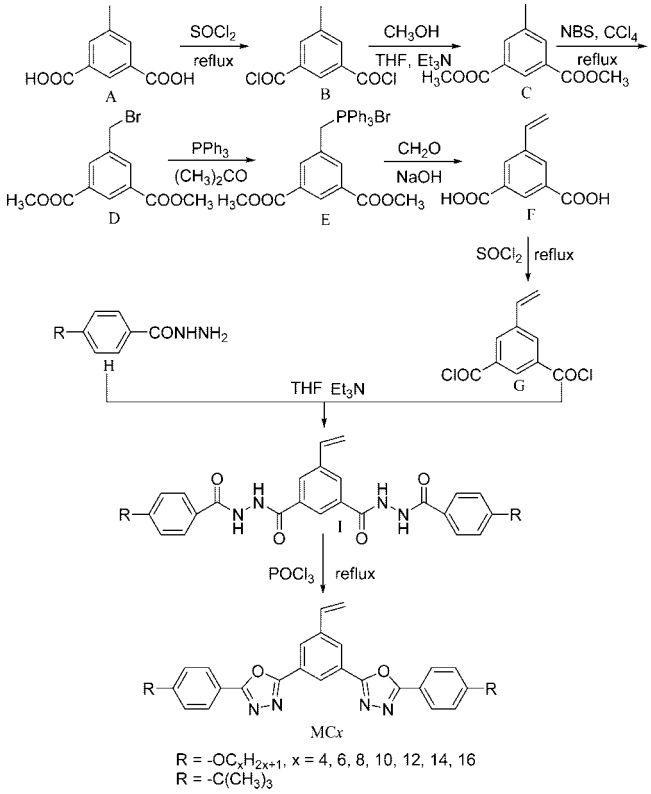

Figure 1. Synthetic routes of MC_x.

Table 1. Synthesis and thermal properties of PC_x

sample	M_n ($\times 10^4$)[a]	PDI[a]	$T_d(N_2)$ (°C)[b]	T_g (°C)[c]
PC_t	12.5	1.33	403	235
PC_4	8.1	1.37	403	186
PC_6	5.6	1.40	398	184
PC_8	7.8	1.43	407	183
PC_{10}	3.7	1.58	399	174
PC_{12}	7.2	1.39	403	172
PC_{14}	5.6	1.46	402	168
PC_{16}	6.3	1.37	395	158

[a] The apparent number-average molecular weight (M_n) and polydispersity (PDI) were measured by GPC using PS standards. [b] The temperatures at 5% weight loss of the samples under nitrogen [$T_d(N_2)$] were measured by TGA heating experiments at a rate of 10 °C/min. [c] The glass transition temperatures were measured by DSC at a heating rate of 20 °C/min under nitrogen atmosphere during the second heating process.

furan (THF) was refluxed over sodium under argon and distilled out before use. Phosphorus oxychloride was distilled before use. Chlorobenzene was washed with H_2SO_4, $NaHCO_3$, and distilled water separately, refluxed over CaH_2 and distilled before use. All other reagents were used as received from commercial sources.

Characterization. ^{1}H NMR spectra were recorded on a BRUKER ARX400 MHz spectrometer using tetramethylsilane as the internal standard at room temperature in chloroform-*d* or dimethyl sulfoxide-d_6.

Elemental analysis was carried out with an Elementar Vario EL instrument.

Gel permeation chromatography (GPC) measurements were carried out on a Waters 2410 instrument equipped with a Waters 2410 RI detector and three Waters μ-Styragel columns (10^3, 10^4, and 10^5 Å), using THF as the eluent at a flow rate of 1.0 mL/min at 35 °C. All GPC data were calibrated with polystyrene standards.

Thermogravimetric analysis (TGA) was performed on a TA SDT 2960 instrument at a heating rate of 10 °C/min in nitrogen atmosphere.

Differential scanning calorimetry (DSC) examination was carried out on a TA DSC Q100 calorimeter with a programmed heating procedure in nitrogen. The sample size was about 10 mg and encapsulated in hermetically sealed aluminum pans, and the pan weights were kept constant. The temperature and heat flow scale at different cooling and heating rates were calibrated using standard materials such as indium and benzoic acid.

Polarized light microscopy (PLM) was carried out to observe the LC textures of the samples on a Leitz Laborlux 12 microscope with a Leitz 350 hot stage.

One-dimensional (1D) wide-angle X-ray diffraction (WAXD) experiments were performed on a Philips X'Pert Pro diffractometer with a 3 kW ceramic tube as the X-ray source (Cu Kα) and an X'celerator detector. Silicon powder and silver behenate were used to calibrate the reflection peak positions at $2\theta > 15°$ and $2\theta < 10°$, respectively. A hot stage (Paar Physica YCU 100) was utilized to study the phase structure evolutions with temperature. The heating and cooling rates in all WAXD experiments were 10 °C/min.

Two-dimensional (2D) WAXD experiments were performed on a Bruker D8Discover diffractometer with GADDS as a 2D detector. Silicon powder and silver behenate were used as standards again. The 2D diffraction patterns were recorded in a transmission mode at room temperature. The oriented samples were prepared by mechanically shearing the films at 280 °C. The sheared film was positioned so that the mechanical shearing direction was either perpendicular or parallel to the point-focused X-ray beam. For both the powder 1D and 2D diffractions, the background scattering was recorded and subtracted from the sample patterns.

Synthesis of Monomers. The synthetic routes of the monomers of 3,5-bis[(4-alkoxyphenyl)-1,3,4-oxadiazole]styrene (MC_x, *x* is the number of carbons in the alkoxy groups, $x = 4$, 6, 8, 10, 12, 14, 16, and t for *tert*-butyl) were depicted in Figure 1. The experimental details are described below using MC_{10} as an example in three steps. Other ^{1}H NMR, mass spectrum, and elemental analysis data of monomers are provided in the Supporting Information.

*(1). Synthesis of Dimethyl 5-Methylbenzene-1,3-dioate (***C***).* A 1.80 g (10 mmol) sample of 5-methylbenzene-1,3-dioic acid (**A**) and 30 mL thionyl chloride was added into a 100 mL round-bottom flask. The mixture was stirred and refluxed for 2 h. After evaporation of the thionyl chloride under reduced pressure, the residue was washed by petrol ester twice and dissolved in anhydrous THF. The obtained light yellow solution of 5-methylbenzene-1,3-dioyl dichloride (**B**) was slowly dropped into an intensely stirred solution of 30 mL methanol and 10 mL triethylamine for 1 h in an ice bath. The solution was further stirred for 12 h at room temperature. After evaporation of the solvent, the residue was washed with water and purified by silica gel column chromatography with dichloromethane as the eluent to obtain dimethyl 5-methylbenzene-1,3-dioate (**C**) as a light yellow solid. Yield: 88%. ^{1}H NMR (δ, ppm): 2.45 (s, 3H, $-CH_3$), 3.94 (s, 6H, $-COOCH_3$), 8.00−8.48 (m, 3H, Ar−H).

*(2). Synthesis of 5-Vinylbenzene-1,3-dioic Acid (***F***).* A 1.92 g (10 mmol) sample of **C**, 1.95 g (11 mmol) of NBS and 0.05 g (0.2 mmol) of BPO were dissolved in 50 mL of carbon tetrachloride.

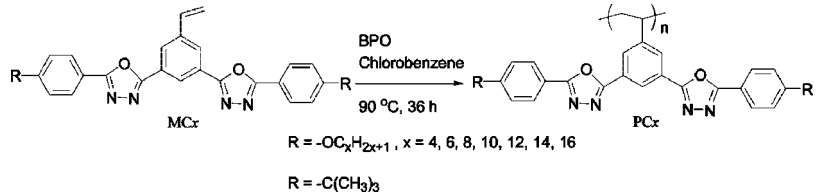

Figure 2. Synthesis of PC_x.

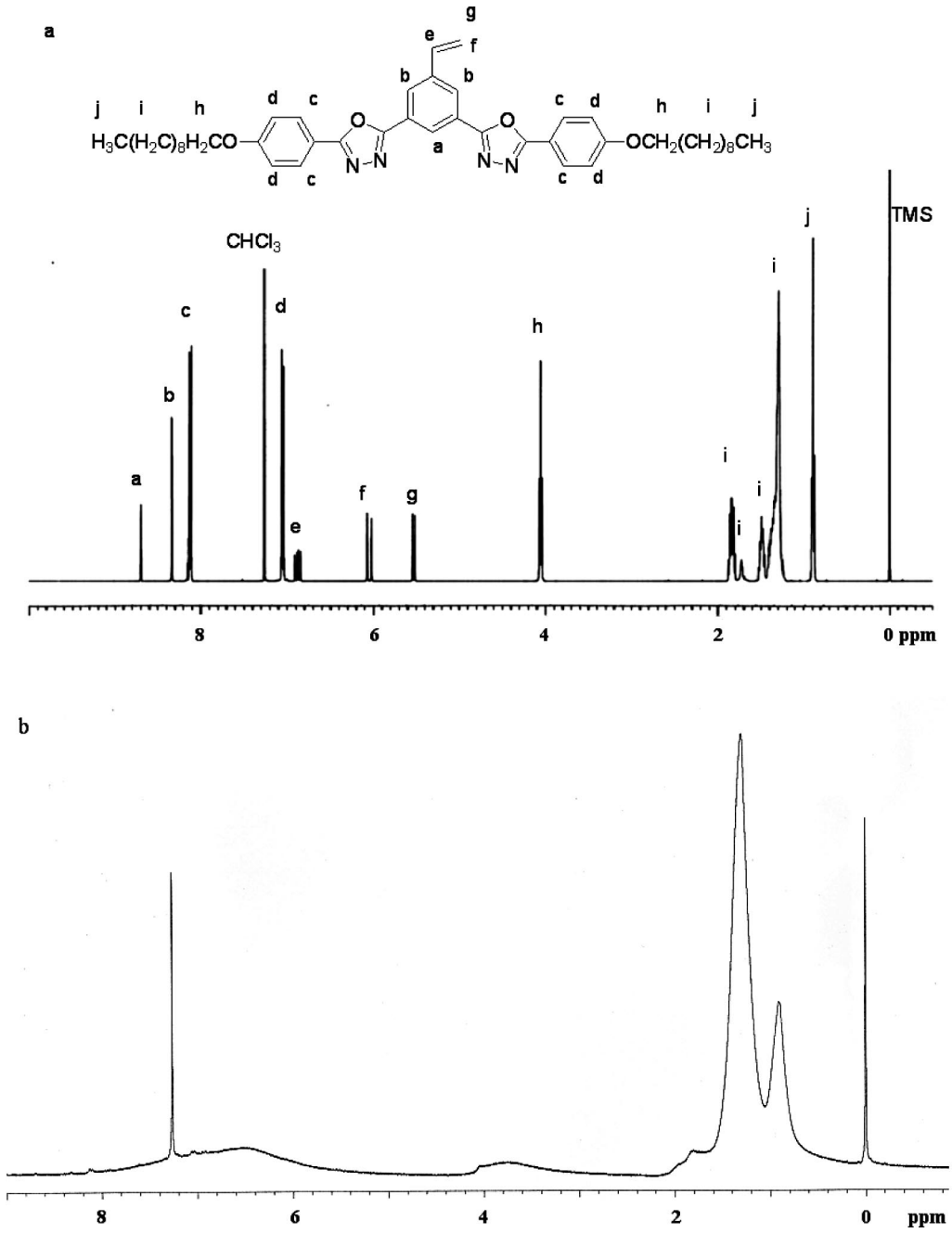

Figure 3. ^{1}H NMR spectrums of MC_{10} (a) and PC_{10} (b) in $CDCl_3$.

The solution was stirred at 60 °C for 2 h and refluxed at 80 °C for 1 h. The floating succinimide was filtrated off and the solvent was evaporated under reduced pressure. Then the residue was boiled with 2.62 g (10 mmol) triphenylphosphine in 30 mL acetone for 3 h. The obtained phosphonium salt was washed by acetone twice. Then, 40 mL of 40% NaOH aqueous solution was slowly dropped into a solution of 50 mL of 40% formaldehyde containing phosphonium salt. The solution was stirred at room temperature for 48 h. After the floating solid was filtrated off, about 100 mL of HCl (4 mol/L) was added into the filtrate. The obtained white solid (**F**) was washed with water several times and dried under reduced pressure to a constant weight. Yield: 60%. ^{1}H NMR(δ, ppm): 2.5 (s, 3H, $-CH_3$) 5.41 (d, 1H, $=CH_2$ trans to the substitute), 5.99 (d, 1H, $=CH_2$ cis to the substitute), 6.93 (q, 1H, $-CH=$), 8.24−8.38(m, 3H, Ar−H), 13.36 (s, 2H, −COOH).

(3). Synthesis of 3,5-Bis[(4-decyloxyphenyl)-1,3,4-oxadiazole]-styrene (MC_{10}). A 1.92 g (10 mmol) sample of 5-vinylbenzene-1,3-dioic acid (**F**) and 30 mL thionyl chloride was added into a 100 mL round-bottom flask. The mixture was stirred and refluxed for 2 h. After evaporation of the thionyl chloride under reduced pressure, the residue was washed by petrol ester twice and dissolved in anhydrous THF. The obtained solution was slowly dropped into 40 mL of anhydrous THF containing 5.53 g of *p*-decyloxybenzhydrazide (20 mmol), 10 mL of triethylamine, and 0.10 g of 2,6-di-*tert*-butyl-4-methylphenol at the temperature of an ice bath. The solution was further stirred at room temperature for 24 h. After evaporation of the solvent, the crude product I was washed with dilute HCl, water, and methanol. A mixture of 6.71 g (9 mmol) **I**, 50 mL of phosphorus oxychloride and 0.10 g of 2,6-di-*tert*-butyl-4-methylphenol was refluxed at 110 °C. The color of reaction changed from yellow to dark green. After cooled, the reaction mixture was slowly poured into excess ice water with intense stirring. The precipitate was washed with water and purified by silica gel column chromatography with dichloromethane and petrol ester (v:v of 10:1) as the eluent to obtain 3,5-bis[(4-decyloxyphenyl)-1,3,4-oxadiazole]styrene (MC_{10}) as a white solid. Yield: 55%.

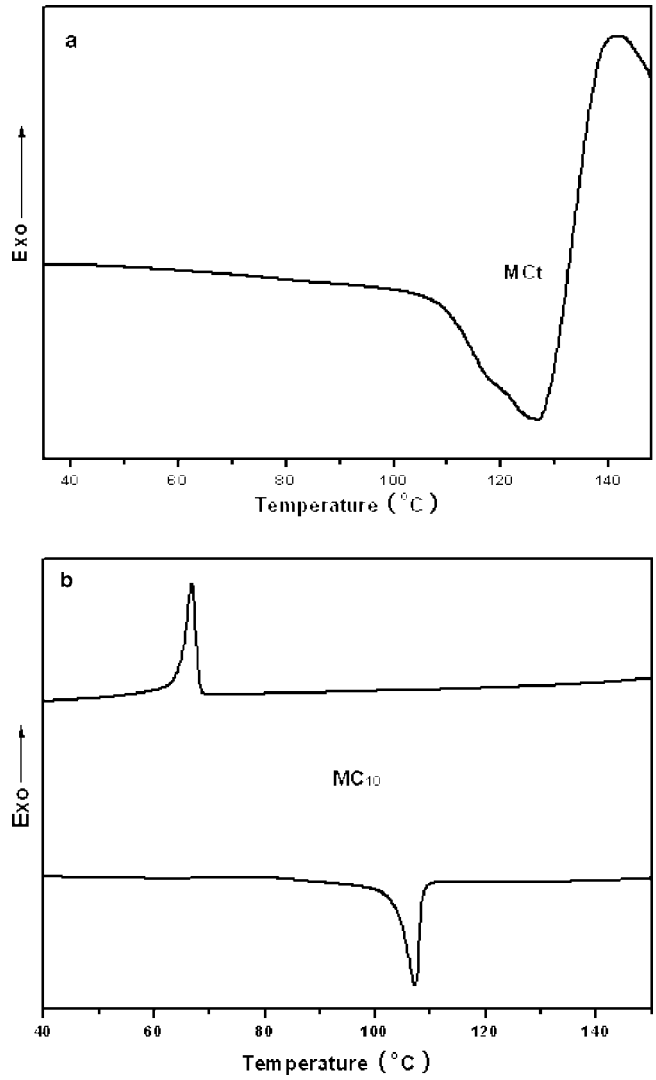

Figure 4. DSC thermograms of MC_t (a) and MC_{10} (b) at a heating and cooling rate of 10 °C /min under nitrogen atmosphere.

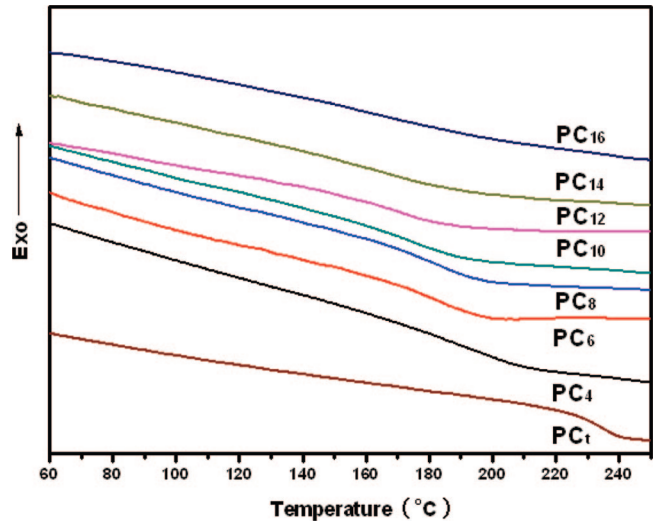

Figure 5. DSC thermograms of PC_x at a heating rate of 20 °C/min under nitrogen atmosphere.

^{1}H NMR (δ, ppm): 0.85−1.88 (m, 38H, alkoxy H), 4.06 (t, 4H, alkoxy H direct connected to oxygen atom), 5.48 (d, 1H, $=CH_2$ trans to the substitute), 6.05 (d, 1H, $=CH_2$ cis to the substitute), 6.88 (q, 1H, $-CH=$), 7.03−8.70(m, 11H, Ar−H).

Mass spectrum (*m*/*e*): 740. Elemental analysis found (calculated for $C_{44}H_{60}N_4O_6$): C, 75.09 (74.97); H, 7.94 (7.95); N, 8.00 (8.01).

Synthesis of Polymers. All polymers (PC_x in Figure 2) were obtained by conventional solution radical polymerization. For example, 0.74 g (1 mmol) of MC_{10}, 100 μL of chlorobenzene solution of 0.05 M BPO, 2 mL of chlorobenzene, and a magnetic stir bar were added into a polymerization tube. After three freeze−pump−thaw cycles, the tube was sealed off under vacuum.

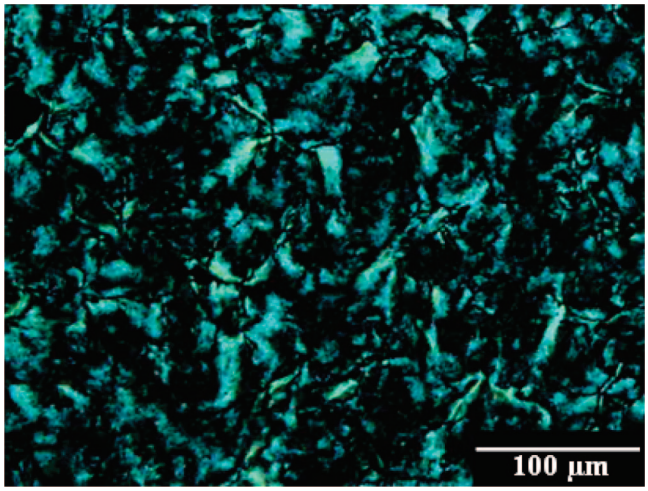

Figure 6. PLM image of PC_{10} taken at 260 °C.

Table 2. Phase structure data of PC_x.

sample	d_{100} (nm)[a]	a (nm)[b]	$L_{side\ group}$ (nm)[c]	sin θ_{100}:sin θ_{110}:sin θ_{200}[a]
PC_4	2.51	2.90	1.44	1.00:1.71:1.95
PC_6	2.74	3.16	1.66	1.00:1.72:1.98
PC_8	3.03	3.50	1.87	1.00:1.73:1.97
PC_{10}	3.23	3.73	2.10	1.00:1.71:1.97
PC_{12}	3.38	3.90	2.32	1.00:1.71:1.99
PC_{14}	3.29	3.80	2.55	1.00:1.74:2.01
PC_{16}	3.46	4.00	2.78	1.00:1.71:1.94
PC_t	3.22	3.72	1.32	1.00:1.72:2.00

[a] Calculated at the temperature of 280 °C for PC_t and 260 °C for other PC_x. [b] Parameter of the hexagonal lattice. [c] Calculated length from the vinyl group to the extended alkoxy end.

Polymerization was carried out at 90 °C for 36 h. The tube was then opened, and the reaction mixture was diluted with THF. The resultant polymer was precipitated and washed with methanol. To eliminate the unreacted monomers, the precipitate was redissolved in THF and then reprecipitated and washed with methanol until no peak was observed at the elution time of monomer in gel permeation chromatography (GPC) measurement. After purification, the polymer was dried to a constant weight. Yield: 58%.

Results and Discussion

Synthesis and Characterization of Monomers and Polymers. The most important compound **F** was obtained by the Wittig reaction. The efficiency of this reaction was improved via washing the floating solid with dilute NaOH aqueous solution several times. To prevent the vinyl group from thermally polymerizing, syntheses of **I** and **M** were carried out in the presence of 2,6-di-*tert*-butyl-4-methylphenol. The precursor of monomer **I** was used after simple purification only because of its poor solubility in common organic solvents.

The structures of monomers and polymers were confirmed by ^{1}H NMR, MS, and IR. As shown in parts a and b of Figure 3, the signals of the vinyl group of MC_{10} at 5.5, 6.0, and 6.8 ppm completely disappeared, indicating the successful polymerization. In addition, the broad peaks of PC_{10} observed indicated the expected polymer structure. The characterization results of PC_x were listed in Table 1.

The apparent number average molecular weights (M_n) of PC_x were about 50 kg/mol and PDIs were about 1.40, which showed good polymerizability of monomers. TGA measurements showed that all polymers were quite stable under nitrogen atmosphere. The temperatures of 5% weight loss (T_d) were around 400 °C as shown in Table 1. The good thermal stability was mainly due to the oxadiazole moiety.[22−24]

Liquid Crystalline Behavior of MC_x and PC_x. All monomers of MC_x were needle-like crystals at room temperature. Upon heating, an endothermic peak followed by an exothermic peak was observed for the MC_t sample as shown in Figure 4a, corresponding to melting and thermal polymerization of monomers, respectively. This phenomenon indicated that the thermal polymerization of MC_t occurred immediately after its melting. Other MC_x samples did not thermal polymerize at their melting point. As shown in Figure 4b, only a melting peak and a crystallization peak were observed during the heating and cooling processes, respectively. PLM was also employed to study the phase transition of MC_x samples (except MC_t). The sample was heated to the temperature about 15 °C below its thermal polymerization temperature and cooled. A bright birefringence was observed at room temperature due to the crystal structure. Upon melting, the monomer sample flowed freely and the birefringence disappeared. Only an isotropic-crystal transition was observed during the cooling process. Compare with other liquid crystalline small molecules with five aromatic rings, a lack of liquid crystallinity in MC_x indicated that the both the mesogen shape and linkage groups between rings played an important role in LC phase formation.[19,21,25,26]

All polymers were amorphous when obtained from solution radical polymerization. The DSC experiments of PC_x were performed under nitrogen atmosphere at the heating and cooling rates of 20 °C /min and 10 °C /min, respectively. Figure 5 showed a set of DSC thermograms of PC_x, and only glass transition could be observed during the second heating process. This phenomenon has been reported in some other MJLCPs with Φ_{NH} and Φ_N phases.[27−29] PC_t had the highest T_g of 234 °C due to the poor mobility of the bulky, rigid end chain. T_g's of other PC_x decreased with the increase in the carbon number of the alkoxy end group, which was different from the results of MJLCPs with rod-like mesogens reported before.[19]

PLM was employed to study the LC behavior of PC_x. The samples were cast from dilute THF solution and slowly dried at room temperature. The liquid crystalline birefringence of PC_{10} was observed upon 260 °C as shown in Figure 6. This temperature was much higher than the glass transition temperature of PC_{10} (174 °C), which was also observed in other PC_x samples. The isotropic phase was not observed even when the temperature reached 320 °C. The birefringence of sample remained when cooled down from liquid crystalline phase to room temperature. This was similar to some MJLCPs reported before.[9,20]

1D WAXD was employed to further investigate the phase structures of PC_x. About 30 mg of polymer was dissolved in THF and cast onto a copper substrate, and then the solvent was allowed to evaporate at room temperature. Parts **a** and **b** of Figure 7 showed two sets of 1D WAXD patterns of PC_6 during the first heating and the subsequent cooling processes, respectively. The intensity of the scattering peak of PC_6 at low 2θ value of 3.3° increased upon the first heating. When the temperature reached 200 °C, two higher-order diffraction peaks were observed. At 260 °C, the position of three diffraction peaks had 2θ values of 3.22, 5.55 and 6.39°. The ratio of scattering vectors of these three peaks was approximately $1:3^{1/2}:4^{1/2}$, indicating a hexagonal columnar structure of the sample PC_6. All these diffraction peaks retained their intensity during the cooling process as some other MJLCPs reported previously. From the maximum d_{100} value (for example, that for PC_6 of 2.74 nm), the hexagonal lattice can therefore be calculated (for PC_6, a = 3.10 nm). Considering the much higher T_g, the 1D WAXD experiments of sample PC_t were performed to a higher temperature of 280 °C. As shown in Figure 7c and 7d, three diffraction peaks with the ratio of scattering vectors of $1:3^{1/2}:4^{1/2}$, indicating that the phase structure was also hexagonal

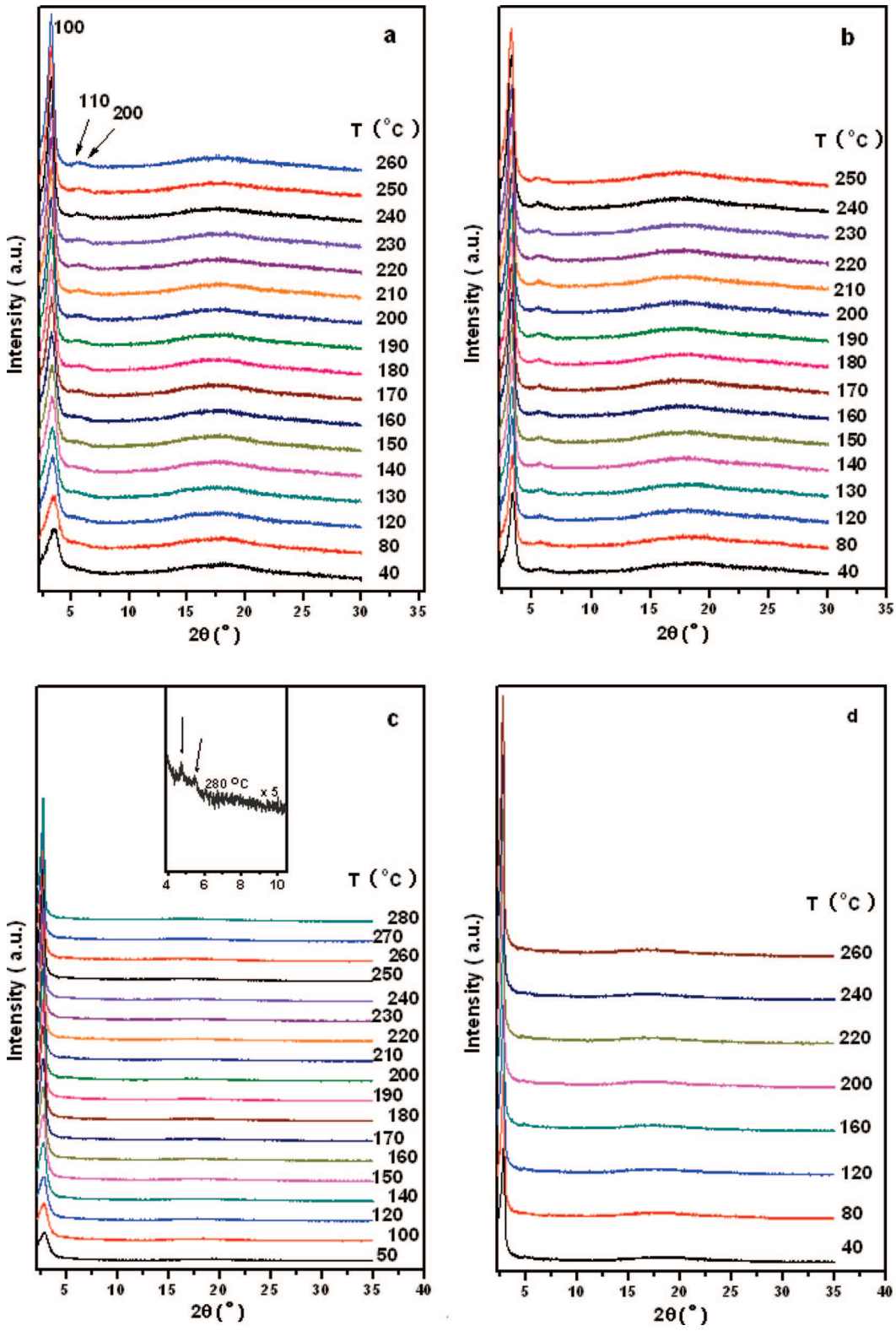

Figure 7. 1D WAXD patterns of PC_6 during the first heating (a) and the subsequent cooling (b). 1D WAXD patterns of PC_t during the first heating (c), the subsequent cooling (d) and partial pattern of PC_t at 280 °C of 2θ from 4° to 10° (inset part of c).

columnar with the d_{100} of 3.22 nm. The low-angle diffraction peak of PC_x slightly shifted toward higher angles during the cooling process as a result of thermal shrinkage. The *d*-spacing values of low-angle diffraction of PC_x as a function of temperature were plotted in Figure 8, and the phase structure data were summarized in Table 2. When the alkoxy end groups were short (for example, PC_4 and PC_6), the hexagonal lattice parameter *a* which indicated the distance between polymer rods was nearly equal to the calculated length of the molecule, indicated the polymer rods packing close to each other. However, when the end groups were longer (for example PC_{10} and PC_{12}), the calculated length were significantly larger than the experimental one. In addition, two unusual phenomena were observed. First, the d_{100} values of PC_x reversed the increasing trend with increasing carbon number of the alkoxy end groups for PC_{14}. Long alkyl tails tend to be in the crystalline state at

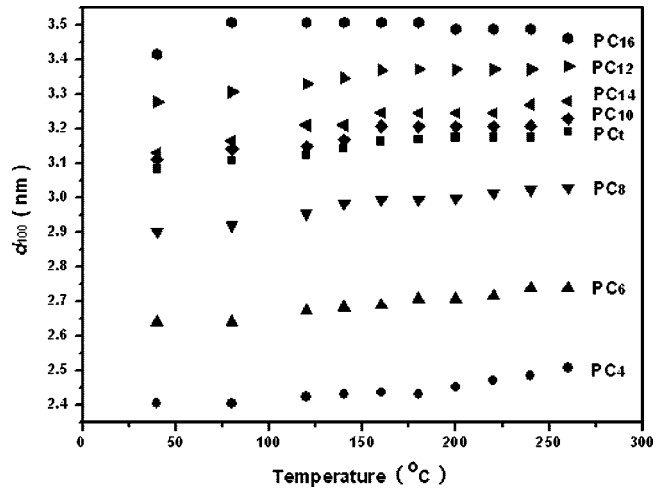

Figure 8. d_{100} values of PC_x as a function of temperature from 40 to 260 °C during the cooling process.

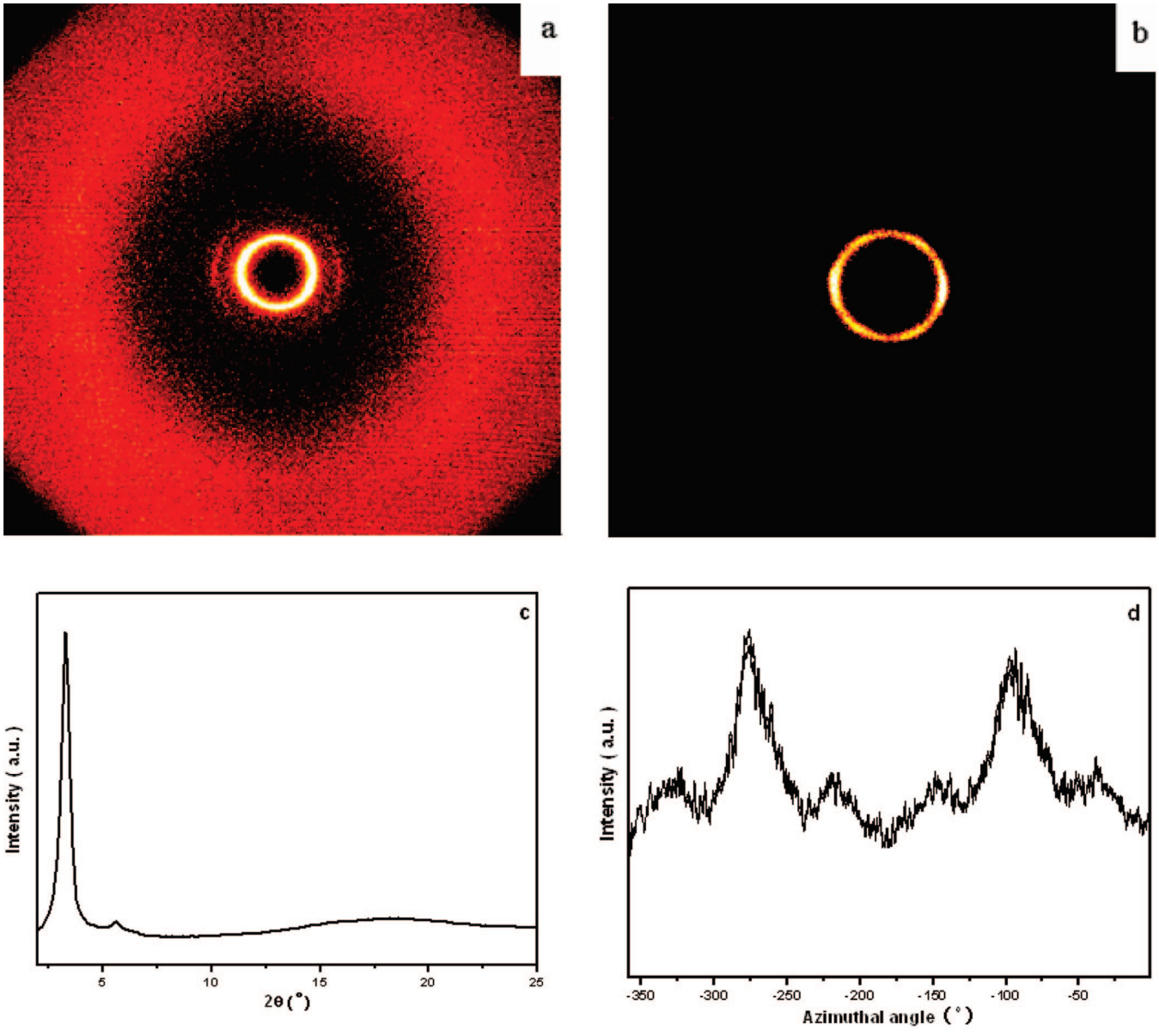

Figure 9. 2D WAXD patterns of PC_6 obtained with the X-ray beam perpendicular (a) and parallel (b) to the shear direction; 2θ integration of (a) along equator (c); azimuthal scan of (b) at $2\theta = 3.3°$ (d).

room temperature. It is possible that if we plot d_{100} vs x (x being the number of carbon atoms in the alkyl tails), there might be two different curves: one for crystalline chains (for PC_{14} and PC_{16}), and one for alkyl chains in isotropic state (for PC_x with

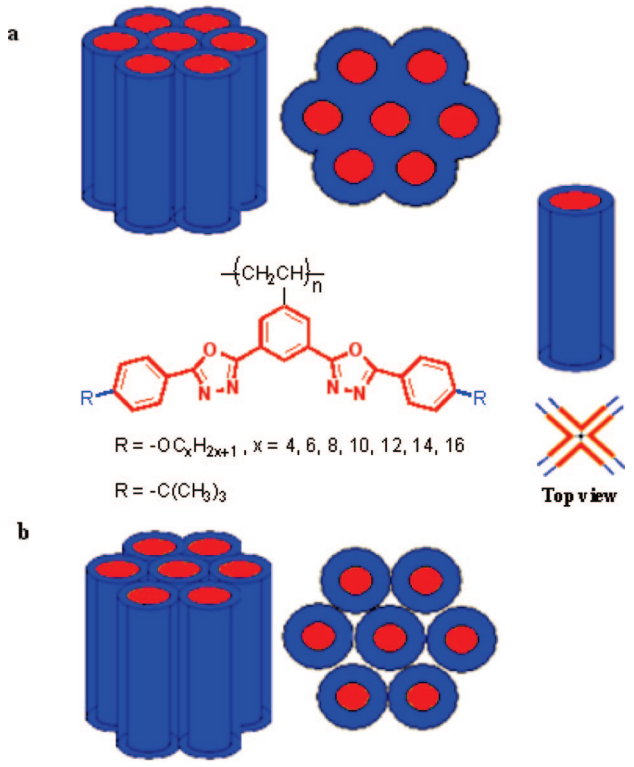

Figure 10. Schematic drawing of the hexagonal columnar packing with (PC_x except PC_t, a) or without (PC_t, b) overlapping of alkoxy tails. (Note that the schematic drawing of the top view did not represent the true positions of the side groups along the polymer backbone, i.e., there was no 4-fold symmetry of the side groups in the projection along the polymer backbone.)

x equal to 4, 6, 8, 10, and 12). Presumably, for alkyl chains with the same *x* number, the crystalline alkyl chains pack more densely, resulting in shorter d_{100}. In addition, such crystallization behavior may change the extent of interdigitation of the alkyl tails. These caused the apparent of irregularity for the parameter *a* of PC_{14}. Second, the d_{100} value of PC_t was approximately equal to that of PC_{10} (note the extended-chain length of the side group of PC_{10} was much longer than that of PC_t), which indicated that they had different packing of polymer rods.

2D WAXD experiments were carried out to confirm the phase structure of PC_x. The sample PC_6 was sheared at a temperature of 300 °C under nitrogen atmosphere and annealed at 200 °C for 24 h. Figure 9a and Figure 9b showed the diffraction patterns with the X-ray beam perpendicular and parallel to the shear direction, respectively. As shown in Figure 9c, two pair of diffraction arcs were clearly observed along the equator and the ratio of scattering vectors of the first and second order diffractions was $1:3^{1/2}$, which indicated that the polymer backbones were parallel to the shear direction with long-range ordered hexagonal packing. When the X-ray incident beam was parallel to the shear direction, six diffraction arcs were observed (Figure 9b). This low-angle diffraction pattern with an azimuthal angle of 60° between two adjacent maxima as shown in Figure 9d confirmed again a hexagonal packing of the polymer rods.

From all these results above, we know that the liquid crystalline phase structures of PC_x were well-defined hexagonal columnar. Compare with MJLCPs having rod-like mesogens, the packing of PC_x greatly changed due to the small difference in chemical shape. In general, the packing of side groups was mainly influenced by two factors, steric hindrance and $\pi-\pi$ interaction.[19−21] However, parallel packing of the bent side groups are not favored when both the $\pi-\pi$ interaction and size of bent side groups are nearly the same as rod-like ones. Thus, there should be another force which leads to the hexagonal packing of the polymer rods. As mentioned above, for all PC_x except PC_t, the d_{100} values were much smaller than the calculated ones. From that, we propose the presence of interpenetrated polymer rods as shown in Figure 10a. The side groups were divided into two parts, the red part for the rigid five-ring structure and blue for flexible tails. When the polymer entered liquid crystalline phase, flexible alkoxy groups extended and interpenetrated with others. This interaction may increase the stability of the structures and lead to the long-range order packing. For PC_t, the large steric hindrance of fully rigid side groups especially the *tert*-butyl groups made the polymer rods difficult to pack closer, which led to the parameter ***a*** larger than the calculated length. In addition, in 1D WAXD patterns, the diffraction halo at the angle of $2\theta = 17-19°$ (*d*-spacing of about 0.5 nm) indicate the short-range ordered structure of side groups. Thus, we propose the packing of PC_t as shown in Figure 10b.

Conclusion

In summary, a series of bent core monomers with different end groups were synthesized. Mesogen-jacketed liquid crystalline polymers were obtained via conventional radical polymerization. The chemical structures of monomers and polymers were confirmed. The monomers did not show liquid crystallinity during both heating and cooling processes. Hexagonal columnar phases were observed when polymers were heated upon their glass transition temperature. Isotropic phase was not observed even at 320 °C. Similar with other MJLCPs, the polymer backbone of PC_x were forced to adopt an extended-chain conformation. Thus, the polymer chain could be regarded as a supramolecular rod. Compared with the fully rigid PC_t, the WAXD results showed the interpenetration of flexible alkoxy groups between polymer rods in other PC_x samples. This research demonstrates that both the molecular shape and chemical structure may influence the packing of polymers. Since the parallel packing of the side groups of PC_x are not favored, MJLCPs with stronger $\pi-\pi$ interaction between bent side groups will be investigated in the future.

Acknowledgment. This research was supported by the National Natural Science Foundation of China (Grant Nos.: 20634010, 20874002, and 20874003).

Supporting Information Available: Tables giving characterization results of MS, elementary analysis, IR, and ^{1}H NMR of the monomers. This material is available free of charge via the Internet at http://pubs.acs.org.

References and Notes

(1) Blumstein, A. *Polymeric Liquid Crystals*; Plenum Press: New York, 1985.
(2) Demus, D.; Goodby, J.; Gray, G. W.; Spiess, H. W.; Vill, V. *Handbook of Liquid Crystals*; Wiley-VCH: Weinheim, Germany, 1998; Vol. 1,Chapter II, p 17.
(3) Finkelmann, H.; Wendorff, H. J. *Structure of Nematic Side Chain Polymers. In Polymeric Liquid Crystals*; Blumstein, A., Ed.; Plenum Press: New York, 1985; p 295.
(4) Zhou, Q. F.; Li, H. M.; Feng, X. D. *Macromolecules* **1987**, *20*, 233.
(5) Zhou, Q. F.; Zhu, X. L.; Wen, Z. Q. *Macromolecules* **1989**, *22*, 491.
(6) Zhou, Q. F.; Wan, X. H.; Zhu, X. L.; Zhang, F.; Feng, X. D. *Mol. Cryst. Liq. Cryst.* **1993**, *231*, 107.
(7) Zhou, Q. F.; Wan, X. H.; Zhu, X. L.; Zhang, D.; Feng, X. D., In *Liquid Crystalline Polymer Systems-Technological Advances*; Isayev, A. I., Kyu, T., Cheng, S. Z. D. Eds.; ACS Symposium Book Series 632; American Chemical Society: Washington, DC, 1996; pp 344−357.
(8) Zhang, D.; Zhou, Q. F.; Ma, Y. G.; Wan, X. H.; Feng, X. D. *Polym. Adv. Technol.* **1997**, *8*, 227.
(9) Zhang, D.; Liu, Y. X.; Wan, X. H.; Zhou, Q. F. *Macromolecules* **1999**, *32*, 5183.
(10) Tu, Y. F.; Wan, X. H.; Zhang, D.; Zhou, Q. F.; Wu, C. *J. Am. Chem. Soc.* **2000**, *122*, 10201.

(11) Tu, Y. F.; Wan, X. H.; Zhang, H. L.; Fan, X. H.; Chen, X. F.; Zhou, Q. F.; Chau, K. *Macromolecules* **2003**, *36*, 6565.
(12) Zhang, H.; Yu, Z.; Wan, X.; Zhou, Q.; Woo, E. M. *Polymer* **2002**, *43*, 2357.
(13) Yu, Z. N.; Wan, X. H.; Zhang, H. L.; Chen, X. F.; Zhou, Q. F. *Chem. Commun.* **2003**, 974.
(14) Yu, Z. N.; Tu, H. L.; Wan, X. H.; Chen, X. F.; Zhou, Q. F. *J. Polym. Sci., Part A: Polym. Chem.* **2003**, *41*, 1454.
(15) Hardouin, F.; Mery, S.; Achard, M. F.; Noirez, L.; Keller, P. *J. Phys. II* **1991**, *1*, 511. Hardouin, F.; Mery, S.; Achard, M. F.; Noirez, L.; Keller, P. *J. Phys. II* **1991**, 871.
(16) Hardouin, F.; Leroux, N.; Mery, S.; Noirez, L. *J. Phys. II* **1992**, *2*, 271.
(17) Kouwer, P. H. J.; Jager, W. F.; Mijs, W. J.; Picken, S. J. *Macromolecules* **2000**, *33*, 4336.
(18) Kouwer, P. H. J.; Jager, W. F.; Mijs, W. J.; Picken, S. J. *Macromolecules* **2002**, *35*, 4322.
(19) Chai, C. P.; Zhu, X. Q.; Wang, P.; Ren, M. Q.; Chen, X. F.; Xu, Y. D.; Fan, X. H.; Ye, C.; Chen, E. Q.; Zhou, Q. F. *Macromolecules* **2007**, *40*, 9361.
(20) Chen, S.; Gao, L.-C.; Zhao, X.-D.; Chen, X.-F.; Fan, X.-H.; Xie, P.-Y.; Zhou, Q.-F. *Macromolecules* **2007**, *40*, 5718.
(21) Chen, X. F.; Tenneti, K. K.; Li, C. Y.; Bai, Y. W.; Zhou, R.; Wan, X. H.; Fan, X. H.; Zhou, Q. F. *Macromolecules* **2006**, *39*, 517.
(22) Hughes, G.; Bryce, M. R. *J. Mater. Chem.* **2005**, *15*, 94.
(23) Wang, C.; Jung, G.-Y.; Batsanov, A. S.; Bryce, M. R.; Petty, M. C. *J. Mater. Chem.* **2002**, *12*, 173.
(24) Cha, S. W.; Choi, S.-H.; Kim, K.; Jin, J.-I. *J. Mater. Chem.* **2003**, *13*, 1900.
(25) Pelzl, G.; Diele, S.; Weissflog, W. *Adv. Mater.* **1999**, *11*, 707.
(26) Weissflog, W.; Nadasi, H.; Dunemann, U.; Pelzl, G.; Diele, S.; Eremin, A.; Kresse, H. *J. Mater. Chem.* **2001**, *11*, 2748.
(27) Ye, C.; Zhang, H. L.; Huang, Y.; Chen, E. Q.; Lu, Y. L.; Shen, D. Y.; Wan, X. H.; Shen, Z. H.; Cheng, S. Z. D.; Zhou, Q. F. *Macromolecules* **2004**, *37*, 7188.
(28) Zhao, Y. F.; Fan, X. H.; Wan, X. H.; Chen, X. F.; Yi, Y.; Wang, L. S.; Dong, X.; Zhou, Q. F. *Macromolecules* **2006**, *39*, 948.
(29) Tang, H.; Zhu, Z. G.; Wan, X. H.; Chen, X. F.; Zhou, Q. F. *Macromolecules* **2006**, *39*, 6887.

MA900125C